Geometric phase in coupled cluster theory

David Williams, Eirik Kjønstad, Todd Martínez

The Journal of Chemical Physics

RESEARCH ARTICLE | JUNE 07 2023

Geometric phase in coupled cluster theory

David M. G. Williams ; Eirik F. Kjønstad ; Todd J. Martínez

J. Chem. Phys. 158, 214122 (2023)
https://doi.org/10.1063/5.0151856

AIP Publishing

The Journal of Chemical Physics ARTICLE scitation.org/journal/jcp

Geometric phase in coupled cluster theory

Cite as: J. Chem. Phys. 158, 214122 (2023); doi: 10.1063/5.0151856
Submitted: 25 March 2023 • Accepted: 15 May 2023 •
Published Online: 7 June 2023

David M. G. Williams, Eirik F. Kjønstad, and Todd J. Martínez[a)]

AFFILIATIONS

Department of Chemistry and the PULSE Institute, Stanford University, Stanford, California 94305, USA
and SLAC National Accelerator Laboratory, 2575 Sand Hill Road, Menlo Park, California 94025, USA

[a)]Author to whom any correspondence should be addressed: Todd.Martinez@stanford.edu

ABSTRACT

It has been well-established that the topography around conical intersections between excited electronic states is incorrectly described by coupled cluster and many other single reference theories (the intersections are "defective"). Despite this, we show both analytically and numerically that the geometric phase effect (GPE) is correctly reproduced upon traversing a path around a defective excited-state conical intersection (CI) in coupled cluster theory. The theoretical analysis is carried out by using a non-Hermitian generalization of the linear vibronic coupling approach. Interestingly, the approach qualitatively explains the characteristic (incorrect) shape of the defective CIs and CI seams. Moreover, the validity of the approach and the presence of the GPE indicate that defective CIs are local (and not global) artifacts. This implies that a sufficiently accurate coupled cluster method could predict nuclear dynamics, including geometric phase effects, as long as the nuclear wavepacket never gets too close to the conical intersections.

I. INTRODUCTION

Coupled cluster (CC) theory[1] can be a highly accurate electronic structure method, but it has well-known shortcomings for nonadiabatic dynamics. As a single reference method, it necessarily breaks down at conical intersections between the ground state and the first excited electronic state.[2] However, CC methods can also fail to describe the potential energy surfaces near intersections between excited states.[3] This is because the description of electronic same-symmetry degeneracies in CC theory is flawed and has a number of well-known non-physical artifacts[4–7] that can only be fully removed by modifying the standard CC equations.[8,9] One such artifact is that conical intersections (CIs), normally characterized by a single point of degeneracy, are replaced by an ellipse of degeneracy, which encloses a domain of complex energies. As a consequence, the corresponding CI seam in nuclear configuration space is qualitatively different, both in shape and dimensionality. For instance, the intersection seam is a tube instead of a curve for triatomic molecules.[6]

Traversing around a CI can lead to a Berry phase[10] or geometric phase[11–13] effect (GPE), which can sometimes have a profound impact on the dynamics of the molecular system.[11,12] Combining this fact with the qualitative change of intersection seams in CC theory raises a fundamental question that has not been addressed in the literature,[4–7] namely, whether traversal around a defective seam still reproduces the expected GPE. The question is not a trivial one, as the presence of multiple CIs is known to alter both the presence and the impact of the GPE, fundamentally affecting, for example, the vibronic level structure of $e \otimes E$ Jahn–Teller systems.[14–24] As such, the impact of traversing a closed loop containing an *infinite* number of degeneracy points instead of a single point of degeneracy requires careful consideration.

One well-established approach for analyzing the GPE is to expand the Hamiltonian matrix up to leading (i.e., linear) order in the vicinity of the CI.[12,13,22] By traversing a closed path around the intersection, one can easily show that the corresponding eigenvectors change sign upon a full rotation about the CI. As will be shown in the present work, this approach lends itself to a generalization to the non-Hermitian Hamiltonian matrices found in CC theory. A similar generalization has been considered for dissipative systems.[25] From this generalization, we demonstrate that the GPE is correctly reproduced in CC theory, implying that defective CIs are local artifacts that need not have a detrimental effect on molecular dynamics far away from defective seams. When viewed from afar, defective seams are indistinguishable from non-defective seams.

Not only does the linear-order expansion approach give an explanation for the GPE, it also explains known qualitative characteristics of defective CIs and CI seams; in particular, it can be shown to explain the tube-like shape of the seam and the "square-root like" shape[5,7] of the potential energy surfaces (PESs)

close to the defect. Another interesting implication is that one can construct a (linear) vibronic coupling Hamiltonian from within the defect and subsequently correct it by imposing a shift on the anti-Hermitian component of the matrix.

This paper is organized as follows. First, we provide an overview of defective CIs (Sec. II). Then we introduce a convenient parametrization of the Hamiltonian (Sec. III) and apply it to explain the seam topography (Sec. IV), the presence of the GPE (Sec. V), as well as the PES topography in planes orthogonal to the seam (Sec. VI).

II. DEFECTIVE CI SEAMS: AN OVERVIEW

In CC theory, several features of two-state degeneracies can be understood[4–6] by considering a general real non-Hermitian 2-by-2 Hamiltonian matrix,

$$\mathbf{H} = \begin{pmatrix} H_{11} & H_{12} \\ H_{21} & H_{22} \end{pmatrix}, \tag{1}$$

and asking what must happen for its eigenvalues to become degenerate. The eigenvalues are given by

$$E_{\pm} = \frac{H_{11} + H_{22}}{2} \pm \frac{1}{2}\sqrt{(H_{22} - H_{11})^2 + 4H_{12}H_{21}}. \tag{2}$$

Before considering the degeneracy, note that since **H** is non-Hermitian, $H_{12}H_{21}$ is able to take on negative values, allowing the term under the square-root to become negative. In this case, $E_{\pm}$ forms a complex conjugate pair of complex eigenvalues. As a consequence, intersections in CC theory are often plagued by non-physical complex energies in the vicinity of near-degeneracies.[3,5]

Additional complications appear at the degeracy itself. When $E_+ = E_-$, **H** becomes non-diagonalizable or *defective*. In other words, the electronic states (the eigenvectors of **H**) collapse onto each other as one approaches the intersection, becoming exactly parallel at the point of degeneracy. Furthermore, the CI seam, defined as the subspace of internal vibrational coordinate space for which $E_+ = E_-$, does not have the correct dimensionality. In fact, whereas Hermitian methods produce degeneracy when *two* conditions are met,[26,27] non-Hermitian methods produce it when only *one* condition is met,[4,6]

$$(H_{22} - H_{11})^2 + 4H_{12}H_{21} = 0. \tag{3}$$

This manifests itself as a defective (N-1)-dimensional intersection tube or cylinder that is folded about a space of dimension N-2, where N is the number of internal coordinates (see Fig. 1). These defective seams persist as long as **H** remains non-diagonalizable, vanishing if and only if the matrix is everywhere diagonalizable in a region containing the CI seam.[6] In CC theory, the Hamiltonian is guaranteed to be diagonalizable at different-symmetry intersections and, of course, in the exact full CC (or full CI) limit.

III. PARAMETERIZING THE HAMILTONIAN

We begin with a useful parameterization of the Hamiltonian matrix **H**:

$$\mathbf{H} = v\mathbf{I} + \mathbf{H}_c = \begin{pmatrix} v & 0 \\ 0 & v \end{pmatrix} + \begin{pmatrix} w & h+a \\ h-a & -w \end{pmatrix}, \tag{4}$$

where **I** is the identity, $\mathbf{H}_c$ is the coupling matrix, and

$$\begin{aligned} v &= \frac{1}{2}(H_{11} + H_{22}), \\ w &= \frac{1}{2}(H_{11} - H_{22}), \\ h &= \frac{1}{2}(H_{12} + H_{21}), \\ a &= \frac{1}{2}(H_{12} - H_{21}). \end{aligned} \tag{5}$$

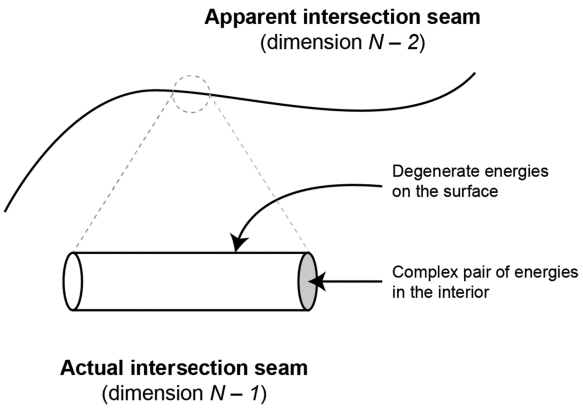

FIG. 1. Intersection seams in coupled cluster theory (N = 3). The intersection seam appears to be a curve (dimension N-2) from a distance, but up close, it is seen to be a tube (dimension N-1) with degenerate eigenvalues on the surface.

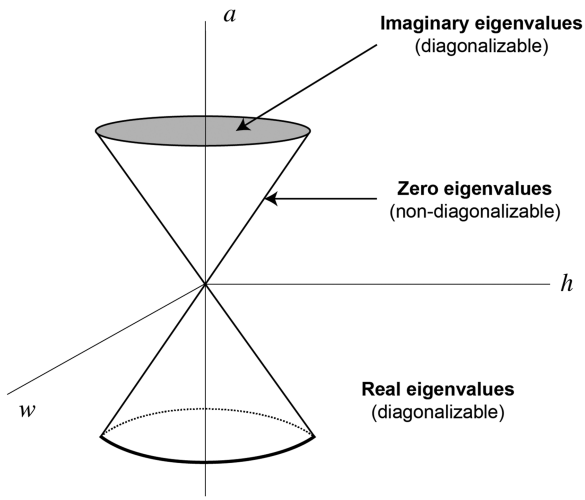

FIG. 2. Eigenvalue regions in Hamiltonian parameter space. The double-cone described by $w^2 + h^2 = a^2$ divides the eigenvalues into three regions: imaginary, zero, and real non-zero. The surface of the cone corresponds to a defective (non-diagonalizable) coupling matrix (except at the origin).

In what follows, we will refer to v and w as the diagonal potential and the diagonal coupling, respectively, and to h and a as the Hermitian and anti-Hermitian coupling, respectively. Of special interest to us are the eigenvectors of $\mathbf{H}$, which are independent of v and identical to the eigenvectors of $\mathbf{H}_c$. Hence, we restrict our attention to $\mathbf{H}_c$, keeping in mind that v only produces a shift in the eigenvalues of $\mathbf{H}_c$ compared to the eigenvalues of the full matrix $\mathbf{H}$.

The eigenvalues of $\mathbf{H}_c$ are given as

$$\lambda_\pm = \pm\sqrt{w^2 + h^2 - a^2}, \tag{6}$$

and they are either real, zero, or purely imaginary,

$$\lambda_\pm \begin{cases} \in \mathrm{R} & w^2 + h^2 > a^2, \\ = 0 & w^2 + h^2 = a^2, \\ \in \mathbb{C} & w^2 + h^2 < a^2. \end{cases} \tag{7}$$

Note in particular that the eigenvalues are real only when the coupling matrix is predominantly Hermitian, that is, when $w^2 + h^2 > a^2$. This provides a useful geometrical picture, separating the different regions in terms of points in the Hamiltonian parameter space (see Fig. 2).

IV. DEFECTIVE CI SEAMS: TOPOGRAPHY

Interestingly, the above-mentioned parametrization of the Hamiltonian sheds light on the topography of defective CIs. Consider a plane in internal coordinate space that bisects an intersection seam in the full CC limit [see Fig. 3(a)]. For sufficiently small displacements away from the seam, the map from internal coordinates to Hamiltonian parameters is linear and, therefore, results in a corresponding plane in Hamiltonian parameter space. In the exact limit, where $\mathbf{H}_c$ is diagonalizable, this plane passes through the origin; otherwise, it would not be diagonalizable. However, when approximations are introduced, the plane may miss the origin and instead bisect the double-cone [see Fig. 3(b)]. In this case, we obtain an elliptic boundary in parameter space that encloses a region with imaginary eigenvalues. We can thus conclude that, in the limit of small enough displacements, the plane bisecting the seam in internal coordinates must also form an elliptic boundary, as the map from nuclear to parameter space (and back) is approximately linear. This explains the defective seam's characteristic tube-like shape and elliptical cross-section.

In the literature, the shape of the seam has been understood by noting that the (N-1)-dimensional subspace must fold in on itself in order to converge, in the full CC limit, to the correct

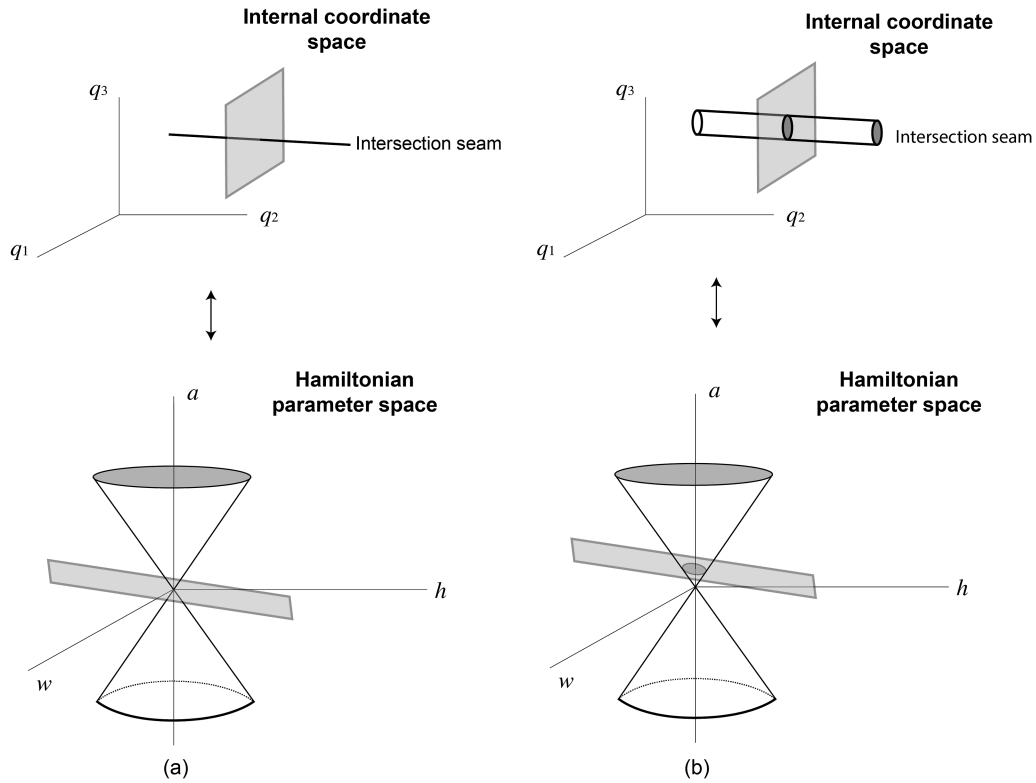

FIG. 3. Plane in internal coordinate space mapped to a plane in Hamiltonian parameter space. We consider small displacements away from the seam, where the map is linear, transforming a plane into a plane. On the left (a), we show the mapping for an everywhere diagonalizable $\mathbf{H}_c$, where the plane passes through the origin in parameter space. On the right (b), the same mapping for a $\mathbf{H}_c$ that is not everywhere diagonalizable, where the plane bisects the cone and leads to a tube-like intersection in the internal coordinate space.

(N-2)-dimensional seam.[6] However, this argument does not show that the seam is expected to be a tube. What this section shows is that a tube-like seam is indeed the shape obtained under the assumption of linear mapping from internal coordinates to Hamiltonian parameters in the vicinity of the CI seam.

The Hamiltonian parameter space also provides a perspective on the similarity constrained CC (SCC) methods introduced by Kjønstad and Koch.[8,9] In the SCC method, the electronic states are required to be orthogonal with respect to a positive-definite metric, implying a diagonalizable $\mathbf{H}_c$. This restricts the space of possible Hamiltonians to the outside of the defective double-cone; in other words, the SCC methods effectively shift planes that bisect the cone to planes that pass through the origin (see Fig. 4). As we have already noted, such a shift can also be imposed in a linear vibronic coupling context by appropriately shifting the anti-Hermitian component of the Hamiltonian matrix.

V. GEOMETRIC PHASE

A. Theory

In the adiabatic picture, traversing around a CI seam can be shown to flip the sign of the electronic wave function upon a full rotation. This feature, known as the geometric phase effect or GPE, is a special case of a Berry phase.[10] As first recognized by Longuet-Higgins,[14,28] a geometric phase implies the existence of at least one point of degeneracy on the surface enclosed by the path. However, the existence of a degeneracy does not imply the existence of a geometric phase. For instance, if the path encloses an even number of degeneracies, there is no geometric phase. This raises the question of whether we should expect a GPE for a path that surrounds a defective intersection, such as the one shown in Fig. 1. The aspect that makes this question non-trivial is that such a path would enclose an infinite number of points of degeneracy (the surface of the tube).

Consider a path surrounding the defective seam in internal coordinate space. Assuming linearity (as discussed in Sec. IV), this path will map to a path surrounding the double-cone in Hamiltonian parameter space, as shown in Fig. 4. To figure out whether there is a geometric phase, we need only consider the eigenvectors along a path that encloses the cone in parameter space.

The eigenvectors of $\mathbf{H}_c$, should they exist, can be expressed (up to phase and normalization $N_\pm$) as

$$\mathbf{v}_\pm = N_\pm \begin{pmatrix} \lambda_\pm - w \\ a - h \end{pmatrix}, \quad \mathbf{H}_c \neq 0. \tag{8}$$

We will only consider paths outside of the double-cone ($\lambda_\pm \in \mathrm{R}$ and $\lambda_\pm \neq 0$), meaning $\mathbf{H}_c$ is ensured to be diagonalizable because $\mathbf{v}_+$ and $\mathbf{v}_-$ are not parallel. Spherical coordinates are a natural choice to describe a loop around the cone,

$$\begin{aligned} a &= r\cos(\phi), \\ w &= r\cos(\theta)\sin(\phi), \\ h &= r\sin(\theta)\sin(\phi). \end{aligned} \tag{9}$$

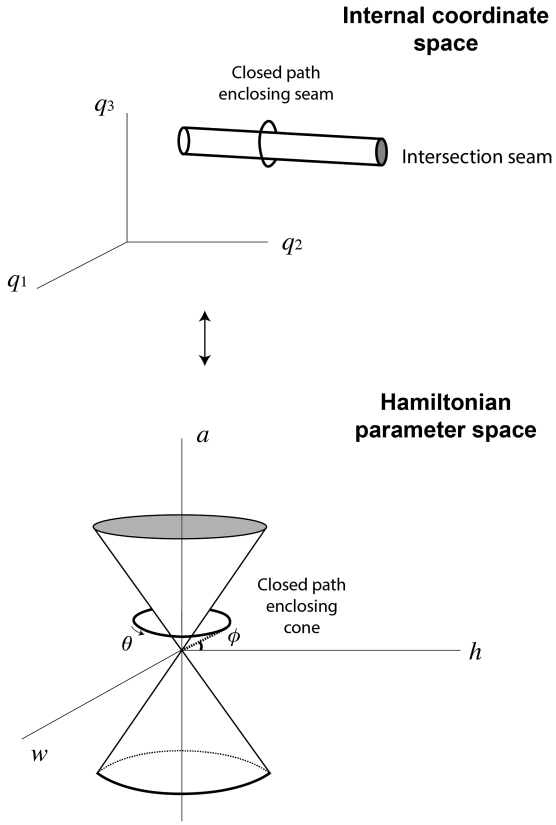

FIG. 4. Closed loop in Hamiltonian parameter space and internal coordinate space about the intersection seam. In parameter space, we consider a loop with a fixed distance from the origin (r) and a fixed elevation angle (φ). The traversal of the closed loop corresponds to varying θ from 0 to 2π.

For this choice, the region with real non-zero eigenvalues satisfies

$$\cos(2\phi) < 0, \quad r > 0, \tag{10}$$

or, in terms of the elevation angle $\varphi = \frac{\pi}{2} - \phi$,

$$|\varphi| < \frac{\pi}{4} = 45^\circ. \tag{11}$$

Without loss of generality, we will now consider a circular path around the double-cone with a fixed elevation angle φ and a fixed distance from the origin r; this path is traced out by varying θ from 0 to 2π. In internal coordinates, this circular path corresponds to an elliptical path around the defective seam.

In spherical coordinates, we have

$$\lambda_\pm = \pm r\sqrt{-\cos(2\phi)} = \pm r\sqrt{\cos(2\varphi)}, \tag{12}$$

and

$$\mathbf{v}_\pm = N_\pm \begin{pmatrix} \pm\sqrt{\cos(2\varphi)} - \cos(\theta)\cos(\varphi) \\ \sin(\varphi) - \sin(\theta)\cos(\varphi) \end{pmatrix}. \tag{13}$$

The normalization factor $N_\pm$ must satisfy

$$\frac{1}{|N_\pm|^2} = 1 - \sin(2\varphi)\sin(\theta) + \cos(2\varphi) \mp 2\sqrt{\cos(2\varphi)}(\cos(\theta)\cos(\varphi)). \quad (14)$$

When the right-hand side is non-zero, Eq. (14) uniquely defines $|N_\pm|$ and we can write

$$N_\pm(\theta,\varphi) = p_\pm(\theta,\varphi)\cdot|N_\pm(\theta,\varphi)|, \quad (15)$$

where $p_\pm$ defines a phase/sign convention for the eigenvectors. For some θ and φ, the right-hand side of Eq. (14) tends to zero, and so $|N_\pm| \to \infty$. However, at these singularities, the normalized eigenvector $\mathbf{v}_\pm$ given by Eq. (13) has a well-defined limit where the vectors are still eigenvectors. This limit can be obtained by applying L'Hôpital's rule or, equivalently, by Taylor expanding the numerator and denominator up to the first order around the singularity, in analogy to the Hermitian case (see Ref. 22). Note that the existence of these limits is guaranteed because the eigenvectors of a matrix can be parameterized as smooth functions of the matrix elements in a small neighborhood about any matrix that has non-degenerate eigenvalues. With an appropriately chosen phase convention, therefore, we can make the eigenvectors in Eq. (13) continuous for all $\theta \in (0, 2\pi)$. One such choice is

$$p_+(\theta,\varphi) = \begin{cases} -\sigma(\theta,\varphi), & \theta \in \left[0, \frac{\pi}{2}\right), \\ \sigma(\theta,\varphi), & \theta \in \left(\frac{3\pi}{2}, 2\pi\right], \\ 1, & \text{otherwise}, \end{cases} \quad (16)$$

and

$$p_-(\theta,\varphi) = \begin{cases} -1, & \theta \in \left[0, \frac{\pi}{2}\right), \\ 1, & \theta \in \left(\frac{3\pi}{2}, 2\pi\right], \\ \sigma(\theta,\phi), & \text{otherwise}, \end{cases} \quad (17)$$

where

$$\sigma(\theta,\varphi) = \text{sgn}(\sin(\varphi) - \sin(\theta)\cos(\varphi)). \quad (18)$$

Now we can easily demonstrate the existence of a geometric phase. Since

$$\sigma(0,\varphi)\sigma(2\pi,\varphi) = \sigma(0,\varphi)^2 = 1, \quad (19)$$

we find that

$$p_\pm(0,\varphi)\cdot p_\pm(2\pi,\varphi) = -1, \quad (20)$$

for any choice of φ outside of the double-cone ($|\varphi| < \pi/4$). Clearly, Eq. (20) implies

$$\mathbf{v}_\pm^T(0,\varphi)\cdot\mathbf{v}_\pm(2\pi,\varphi) = -1, \quad (21)$$

and confirms the presence of a geometric phase for arbitrary closed paths around the double-cone in parameter space (see Fig. 5) and, therefore, any closed path around a defective intersection seam in internal coordinate space.

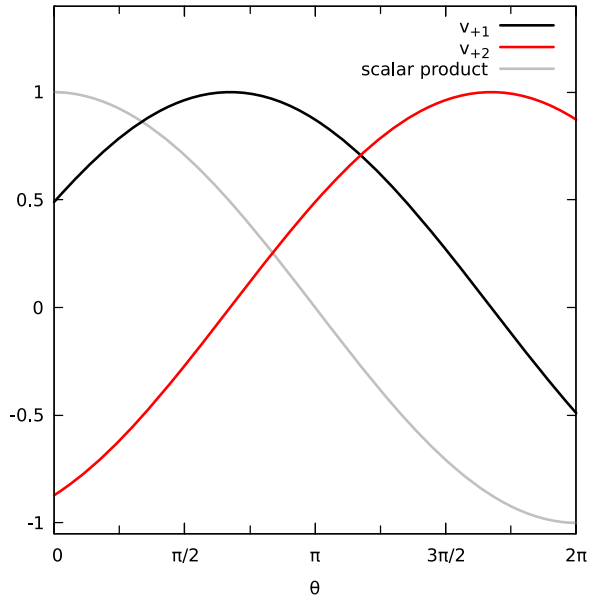

FIG. 5. Geometric phase effect around a defective conical intersection for a representative example path. Red/black: Components of the eigenvector $\mathbf{v}_+$ as a function of θ along a circular path. Gray: Scalar product of $\mathbf{v}_+^T(0)\mathbf{v}_+(\theta)$, showing a sign flip after a full rotation.

B. Numerical example: geometric phase effect in CCSD

This fact is also easily demonstrated numerically. Here, we consider the $2^1A'/3^1A'$ intersection seam in hypofluorous acid (HOF), which has been thoroughly studied and mapped out in earlier work by two of the authors.[6] As our plane is in internal coordinate space, we fix the OH bond length to $R_{OH} = 1.09$ Å and allow the OF bond length (R_{OF}) and the OHF angle (θ_{HOF}) to vary. Next, we construct a loop by defining polar coordinates (r,θ) in the (R_{OF},θ_{HOF}) plane, taking the origin to be

$$R_{OF}^0 = 1.3060 \text{ Å}, \quad \theta_{HOF}^0 = 91^\circ = 1.588 \text{ rad}. \quad (22)$$

Specifically, we let the radius be $r_0 = 0.005$ and define an elliptical loop through

$$\theta_{HOF} = \theta_{HOF}^0 + \gamma\, r_0 \cos(\theta), \quad R_{OF} = R_{OF}^0 + r_0 \sin(\theta), \quad (23)$$

where $\theta \in [0, 2\pi)$ and $\gamma = 10$. In our calculations, we let θ vary from 0 to 2π and track the dominant excited state amplitudes of the $2^1A'$ state given by EOM-CCSD/aug-cc-pVDZ. Calculations were performed with the electronic structure program e^T, version 1.9.[29]

Figure 6 follows the seven largest amplitudes around the loop for $\theta = 0$. The amplitudes flip as we traverse the loop, demonstrating the geometric phase effect at the EOM-CCSD level of theory.

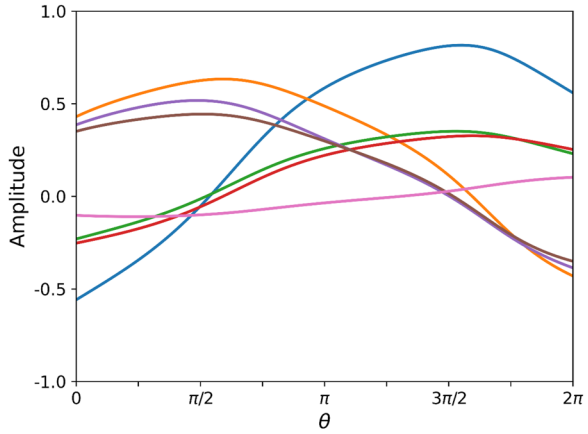

FIG. 6. Geometric phase effect in coupled cluster theory (EOM-CCSD). The dominant amplitudes of the $2^1A'$ state in HOF are shown as a function of the loop angle θ surrounding the $2^1A'/3^1A'$ intersection seam.

VI. DEFECTIVE BRANCHING PLANES: TOPOGRAPHY

As one approaches the defective CI, the potential energy curves are observed to have a characteristic square-root like shape.[4–7] This fact was recently revisited and analyzed.[7] Here, we will show how this feature appears when treating all the coupling terms in leading order. In particular, we will see that the intersecting PESs assume the shape of deformed hyperboloids in planes approximately orthogonal to the defective intersection seam (branching planes).

Using the parameterization defined in Sec. III, we can reason about the shape of the PESs in such planes from corresponding planes in Hamiltonian parameter space. In the vicinity of the seam, the branching plane in parameter space corresponds to skewed and rotated branching planes in nuclear coordinate space.

As a must remain nonzero near a defective CI as w and h vanish, we find that the plane from Fig. 3 intersects the a axis at some $a_0 \neq 0$. This corresponds to a leading zeroth order term in a at an expansion point within the defective domain of nuclear configuration space. Therefore, let us first, for the sake of simplicity, consider only the leading order, $a = a_0$. The eigenvalues $\lambda_\pm$ of $\mathbf{H}_c$ then simplify to rotationally symmetric functions of w and h,

$$\lambda_\pm = \pm\sqrt{w^2 + h^2 - a_0^2}. \tag{24}$$

Their combined graph satisfies the parametric equation

$$w^2 + h^2 - \lambda^2 = a_0^2, \tag{25}$$

which is a hyperboloid centered around the energy axis λ. Comparing an analytical hyperboloid to the observed topography for an EOM-CCSD calculation, we see that they are practically identical (see Fig. 7).

So far, we have considered a to be of the zeroth order for simplicity. If we consider a to be of first order, that is, if we tilt the plane in parameter space, we simply deform the defective circular boundary to an ellipse, and the PESs become deformed hyperboloids. Therefore, treating a as the first order does not significantly change the picture.

From the hyperboloidal shape of the PESs in Eq. (24), we can readily infer the asymptotic square-root like behavior near the degeneracy. By expanding $r = \sqrt{w^2 + h^2}$ about the point of degeneracy $r = a_0$, we find that

$$\begin{aligned}\lambda_\pm &= \pm\sqrt{r^2 - a_0^2} \\ &= \pm\sqrt{(a_0 + \varepsilon)^2 - a_0^2} \\ &= \pm\sqrt{2a_0\varepsilon + \varepsilon^2} \approx \pm\sqrt{2a_0\varepsilon},\end{aligned} \tag{26}$$

for sufficiently small ε. As shown by Thomas *et al.*, this behavior can alternatively be seen through series expansions in fractional powers of some distance ε from the degeneracy.[7] Here, we find the same result from a generalized linear vibronic coupling Hamiltonian.

Note also that when $a_0 \ll \varepsilon$, Eq. (26) once again becomes linear in ε, recovering the behavior of a conical intersection for very small a_0 or far away from the degeneracy. A defective CI, therefore, appears conical (i.e., linear) to a wave packet that is sufficiently far away from the defective region.

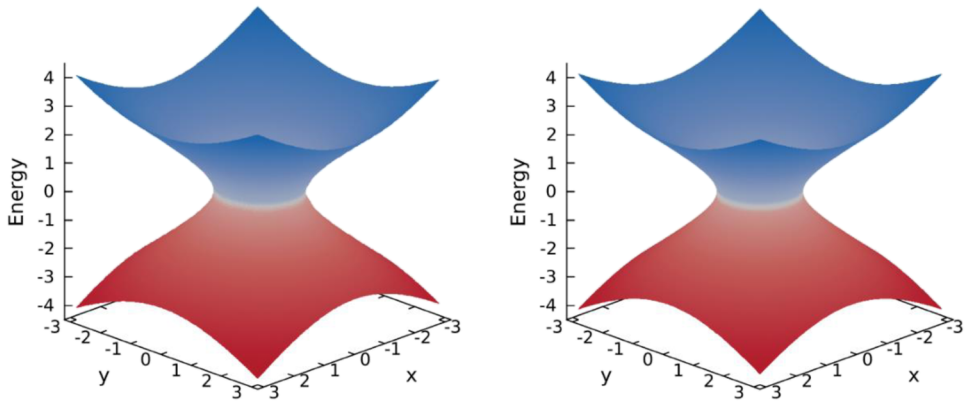

FIG. 7. Branching plane PES topography with EOM-CCSD (left) and VC Hamiltonian (right). The EOM-CCSD plane is spanned by the internal coordinates R_{OF} and θ_{HOF} (at R_{OH} = 1.09 Å) for the $2^1A'/3^1A'$ intersection in HOF. These coordinates are scaled and rotated into arbitrary units to coincide with the VC Hamiltonian. The energy difference is also scaled and given in arbitrary units. See the Appendix for rotation and scaling parameters.

VII. CONCLUSIONS

The characteristic features of defective conical intersections (CIs) in coupled cluster theory were studied in the present work. Although we have focused on coupled cluster theory, similar defects occur in other single reference theories, such as time-dependent density functional theory.[2] Therefore, our conclusions are transferable to these other methods with at most minor changes. Of course, Hermitian theories, including ADC(2),[30] do not exhibit these kinds of defects.

By adapting the standard linear vibronic coupling scheme to the non-Hermitian case, we showed that the geometric phase effect is reproduced in the case of defective CIs. This finding was also reproduced numerically. We also showed that other features of defective CIs, such as the tube-like shape of the seam and the square-root like shape of the energy surfaces near the defect, are qualitatively reproduced to leading order. This provides straightforward explanations of these features in the language of vibronic coupling theory.

Despite the presence of ill-behaved domains of nuclear configuration space yielding complex energies, the fundamental properties of defective CIs can be understood straightforwardly in the limit of small displacements, requiring coupling terms only up to linear order. This suggests that defective CIs can be understood and analyzed utilizing pictures from well-established vibronic coupling theory. In particular, using a coupling Hamiltonian that is of linear order as a function of the nuclear coordinates, we found that the domain of complex eigenvalues must form an ellipse for any given branching plane, explaining the characteristic tube-like shape of defective seams. The same analysis also reproduces the observed topography of defective CIs, identifying the square-root like shape to resemble a deformed hyperboloid near the defect. Note that, far from the defective CI, hyperboloids resemble the physically correct double cone profile. Furthermore, the linear vibronic coupling Hamiltonian explains the existence of a geometric phase, despite the fact that a closed path around the seam encloses infinitely many degeneracies instead of one.

This result was also confirmed numerically. As a consequence, it is reasonable to expect that even in the presence of defective CIs, nuclear dynamics will remain qualitatively correct as long as the nuclear wavepacket is sufficiently far away from the seam. This implies that defects produce purely local artifacts without introducing global artifacts to the PESs. This indicates that despite the defective regions, coupled cluster methods might be capable of providing a qualitatively correct description of quantum dynamics involving excited state CIs, as long as the wavepacket never ventures into the defective regions. Of course, simulating dynamics involving ground state CIs remains problematic due to the single-reference description of the CC ground state.

Capturing dynamics passing through (or too close to) a defect would still require a diagonalizable CC method, such as similarity constrained CC. As the present work indicates, diagonalizability can also be obtained in the generalized vibronic coupling case by imposing an appropriate shift of the anti-Hermitian component of the Hamiltonian. Furthermore, the fact that the GPE is reproduced suggests that the effects of defective CIs are not global, motivating further investigations of nonadiabatic dynamics with coupled cluster theory.

ACKNOWLEDGMENTS

This work was supported by the AMOS program of the U.S. Department of Energy, Office of Science, Basic Energy Sciences, Chemical Sciences, and Biosciences Division. E.F.K. acknowledges funding from the Research Council of Norway through FRINATEK Project No. 275506. We acknowledge computing resources through UNINETT Sigma2, the National Infrastructure for High Performance Computing and Data Storage in Norway through Project No. NN2962k.

AUTHOR DECLARATIONS

Conflict of Interest

The authors have no conflicts to disclose.

Author Contributions

David M. G. Williams: Conceptualization (equal); Formal analysis (equal); Investigation (equal); Validation (equal); Writing – original draft (equal); Writing – review & editing (equal). **Eirik F. Kjønstad**: Conceptualization (equal); Investigation (equal); Software (equal); Validation (equal); Visualization (equal); Writing – original draft (equal); Writing – review & editing (equal). **Todd J. Martínez**: Conceptualization (equal); Formal analysis (equal); Funding acquisition (equal); Resources (equal); Supervision (equal); Validation (equal); Writing – original draft (supporting); Writing – review & editing (equal).

DATA AVAILABILITY

The data that support the findings of this study are available within the article.

APPENDIX: EOM-CCSD PLANE COORDINATES

To obtain a parametrization of the branching plane comparable to the analytic model in Fig. 7, the physical HOF coordinates R_{OF} and θ_{HOF} need to be shifted, rotated, and scaled appropriately. Defining the displacement coordinates

$$\begin{aligned} R &= (R_{\mathrm{OF}} - R_0) \cdot \text{Å}^{-1}, \\ \theta &= (\theta_{\mathrm{HOF}} - \theta_0) \cdot \mathrm{rad}^{-1}, \end{aligned} \tag{A1}$$

where $R_0 = 1.306\,059$ Å and $\theta_0 = 1.588\,686$ rad, we can express the rotated coordinates x, y that were used in Fig. 7 as

$$\begin{aligned} x &= a_x(\cos(\varphi)R + \sin(\varphi)\theta), \\ y &= a_y(-\sin(\varphi)R + \cos(\varphi)\theta), \end{aligned} \tag{A2}$$

where $\varphi = 1.6$ rad, $a_x = 200$, and $a_y = 2000$, respectively. The energy axis was also scaled by an arbitrary factor of 2400 inverse Hartree to obtain energy ranges comparable to the model.

REFERENCES

[1] R. J. Bartlett and M. Musiał, "Coupled cluster theory in quantum chemistry," Rev. Mod. Phys. **79**, 291 (2007).
[2] B. G. Levine, C. Ko, J. Quenneville, and T. J. MartÍnez, "Conical intersections and double excitations in time-dependent density functional theory," Mol. Phys. **104**, 1039 (2006).
[3] F. Plasser, R. Crespo-Otero, M. Pederzoli, J. Pittner, H. Lischka, and M. Barbatti, "Surface hopping dynamics with correlated single-reference methods: 9H-Adenine as a case study," J. Chem. Theory Comput. **10**, 1395 (2014).
[4] C. Hättig, "Structure optimizations for excited states with correlated second-order methods," Adv. Quantum Chem. **50**, 37 (2005).
[5] A. Köhn and A. Tajti, "Can coupled-cluster theory treat conical intersections?," J. Chem. Phys. **127**, 044105 (2007).
[6] E. F. Kjønstad, R. H. Myhre, T. J. Martinez, and H. Koch, "Crossing conditions in coupled cluster theory," J. Chem. Phys. **147**, 164105 (2017).
[7] S. Thomas, F. Hampe, S. Stopkowicz, and J. Gauss, "Complex ground-state and excitation energies in coupled-cluster theory," Mol. Phys. **119**, e1968056 (2021).
[8] E. F. Kjønstad and H. Koch, "Resolving the notorious case of conical intersections for coupled cluster dynamics," J. Phys. Chem. Lett. **8**, 4801 (2017).
[9] E. F. Kjønstad and H. Koch, "An orbital invariant similarity constrained coupled cluster theory," J. Chem. Theory Comput. **15**, 5386 (2019).
[10] M. V. Berry, "Quantal phase factors accompanying adiabatic changes," Proc. R. Soc. London, Ser. A **392**, 45 (1984).
[11] W. Domcke, D. R. Yarkony, and H. Koppel, *Conical Intersections: Electronic Structure, Dynamics and Spectroscopy* (World Scientific, Singapore, 2004).
[12] C. A. Mead, "The geometric phase in molecular systems," Rev. Mod. Phys. **64**, 51 (1992).
[13] D. R. Yarkony, "Diabolical conical intersections," Rev. Mod. Phys. **68**, 985 (1996).
[14] H. C. Longuet-Higgins, U. Opik, M. H. L. Pryce, and R. A. Sack, "Studies of the Jahn-Teller effect. II. The dynamical problem," Proc. R. Soc. London, Ser. A **244**, 1 (1958).
[15] R. Englman, *The Jahn-Teller Effect in Molecules and Crystals* (Wiley-Interscience, New York, 1972).
[16] M. C. M. O'Brien, "The dynamic Jahn-Teller effect in octahedrally coordinated d^9 ions," Proc. R. Soc. London, Ser. A **281**, 323 (1964).
[17] C. Alden Mead, "The molecular Aharanov-Bohm effect in bound states," Chem. Phys. **49**, 23 (1980).
[18] F. S. Ham, "Berry's geometrical phase and the sequence of states in the Jahn-Teller effect," Phys. Rev. Lett. **58**, 725 (1987).
[19] J. W. Zwanziger and E. R. Grant, "Topological phase in molecular bound states: Application to the E⊗e system," J. Chem. Phys. **87**, 2954 (1987).
[20] J. W. Zwanziger, M. Koenig, and A. Pines, "Berry's phase," Annu. Rev. Phys. Chem. **41**, 601 (1990).
[21] J. Schön and H. Koppel, "Geometric phase effects and wave packet dynamics on intersecting potential energy surfaces," J. Chem. Phys. **103**, 9292 (1995).
[22] T. Weike, D. M. G. Williams, A. Viel, and W. Eisfeld, "Quantum dynamics and geometric phase in E ⊗ e Jahn-Teller systems with general C_{nv} symmetry," J. Chem. Phys. **151**, 074302 (2019).
[23] R. Baer, D. M. Charutz, R. Kosloff, and M. Baer, "A study of conical intersection effects on scattering processes: The validity of adiabatic single-surface approximations within a quasi-Jahn-Teller model," J. Chem. Phys. **105**, 9141 (1996).
[24] D. R. Yarkony, "Nuclear dynamics near conical intersections in the adiabatic representation: I. The effects of local topography on interstate transitions," J. Chem. Phys. **114**, 2601 (2001).
[25] J. C. Garrison and E. M. Wright, "Complex geometrical phases for dissipative systems," Phys. Lett. A **128**, 177 (1988).
[26] J. von Neumann and E. P. Wigner, "On the behavior of eigenvalues in adiabatic processes," Phys. Z. **30**, 467–470 (1929).
[27] E. Teller, "The crossing of potential energy surfaces," J. Phys. Chem. **41**, 109 (1937).
[28] H. C. Longuet-Higgins, "The intersection of potential energy surfaces in polyatomic molecules," Proc. R. Soc. A **344**, 147 (1975).
[29] S. D. Folkestad, E. F. Kjønstad, R. H. Myhre, J. H. Andersen, A. Balbi, S. Coriani, T. Giovannini, L. Goletto, T. S. Haugland, A. Hutcheson, I.-M. Høyvik, T. Moitra, A. C. Paul, M. Scavino, A. S. Skeidsvoll, Å. H. Tveten, and H. Koch, "e^T 1.0: An open source electronic structure program with emphasis on coupled cluster and multilevel methods," J. Chem. Phys. **152**, 184103 (2020).
[30] A. Dreuw and M. Wormit, "The algebraic diagrammatic construction scheme for the polarization propagator for the calculation of excited states," WIRES Comput. Mol. Sci. **5**, 82–95 (2015).